

## Concept of radius of gyration in general relativity

M. A. Abramowicz

*NORDITA, Blegdamsvej 17, DK-2100 Copenhagen, Denmark  
and International Centre for Theoretical Physics, Strada Costiera 11, I-34014 Trieste, Italy*

J. C. Miller

*Osservatorio Astronomico di Trieste, Via Tiepolo 11, I-34131 Trieste, Italy;  
Scuola Internazionale Superiore di Studi Avanzati, Strada Costiera 11, I-34014 Trieste, Italy;  
and Department of Physics, University of Oxford, England*

Z. Stuchlík

*Department of Physics, Silesian University of Opava, Bezručovo nám. 13, 74601 Opava, Czechoslovakia\*  
and Department of Physics, Queen Mary & Westfield College, University of London, England*

(Received 1 September 1992)

The radius of gyration is a familiar concept in Newtonian mechanics and a suitably defined relativistic generalization of it turns out to be very useful for analyzing rotational effects in strong gravitational fields. The present paper contains a discussion of the properties of this quantity and of its level surfaces (the von Zeipel cylinders) and also of its connection with the effective potential for photon motion and with ideas of centrifugal force. The direction of increase of the radius of gyration gives a preferred determination of the local outward direction relevant for the dynamical effects of rotation, but this direction becomes misaligned with the *global* outward direction in strong-field situations. This misalignment underlies some apparently counterintuitive behavior of the centrifugal force in strong fields which has recently been the subject of considerable interest.

PACS number(s): 04.20.Cv, 95.30.Lz, 97.60.Sm

### I. INTRODUCTION

In Newtonian mechanics, the idea of radius of gyration is a familiar one in connection with the rotational properties of rigid bodies. It is defined as the radius of the circular path on which a pointlike particle having the same mass and angular velocity as the rigid body would also have the same angular momentum; in other words, it is the value of  $\bar{r}$  given by the equation

$$J = M\bar{r}^2\Omega, \quad (1)$$

where  $J$  is the angular momentum,  $M$  is the mass, and  $\Omega$  is the angular velocity, so that

$$\bar{r} = \left[ \frac{J}{M\Omega} \right]^{1/2}. \quad (2)$$

For a point particle moving along a circle, the value of  $\bar{r}$  given by Eq. (2) is (trivially) just the ordinary radius of the circle.

In general relativity, things are more complicated because there is more than one satisfactory way of measuring the radius of a circle. Two standard measures are the *circumferential radius* (the proper circumference divided by  $2\pi$ ) and the *radial proper distance*. If a generalization

of Eq. (2) is used as the definition of  $\bar{r}$  for a point particle moving along the circle, then this provides a third measure. We use the generalization

$$\bar{r} = \left[ \frac{\mathcal{L}}{\mathcal{E}\Omega} \right]^{1/2}, \quad (3)$$

where  $\mathcal{L}$  is the angular momentum of the particle and  $\mathcal{E}$  is its energy. Whereas in Newtonian theory these three ways of measuring radius give results which are identical, in general relativity they are distinct. We propose that  $\bar{r}$  is the right quantity to use for discussing the dynamical effects of rotation and that the direction of increase of  $\bar{r}$  defines the *local outward direction* relevant for this purpose. It turns out that when formulas are written in terms of  $\bar{r}$ , a very simple and elegant unified picture emerges.

The level surfaces of  $\bar{r}$ , defined as above, are the *von Zeipel cylinders*, which were first discussed in the context of general relativity by Abramowicz [1] and have since proved to be a very useful concept for analyzing the behavior of rotating fluids in axially symmetric, stationary space-times. They are normally introduced as surfaces on which the ratio ( $\mathcal{L}/\Omega$ ) is constant (where  $\mathcal{L}$  is the specific angular momentum  $\mathcal{L}/\mathcal{E}$ ), but it now seems more obvious to speak of them as the surfaces on which the radius of gyration is constant. In Newtonian theory, they are ordinary straight cylinders, but in general relativity their shape becomes more complicated as they are distorted by space-time curvature and it is even possible for

\*Permanent address.

their topology to be noncylindrical.<sup>1</sup> Knowledge of this and of the resulting consequences is an important key for understanding rotational effects in general relativity.

As recently emphasized by de Felice [4], in strong-field situations, it can become unclear which directions should properly be identified as the “inward” and “outward” ones. What should be done depends on the context [5]. From a “global” point of view, the outward direction is the direction of increase of the proper circumference of concentric circles, but for rotational purposes the outward direction should be identified with the local direction of increase of  $\bar{r}$  (i.e., with the outward normal to the von Zeipel cylinders).

For the main part of this paper, we will restrict our discussion to the case of motion in a background space-time which is static and axially symmetric. Generalization to the case of a stationary space-time is straightforward, however, and has already been completed. Extension to completely general space-times is presently under investigation. Some parts of the present discussion have been foreshadowed in an earlier paper by Abramowicz [3], but more details are given here within a unified approach. In Sec. II, we review briefly the argument given by Abramowicz when introducing his proposed definition of centrifugal force in general relativity. This definition is seen to fit very naturally within the present discussion. In Sec. III, we demonstrate a surprising connection between the radius of gyration and the effective potential for photon motion. The equatorial effective potential curve and the form of the von Zeipel cylinders for the case of a vacuum Schwarzschild (black-hole) space-time are already well known (see, for example, Shapiro and Teukolsky [6] for the former and Abramowicz [3] for the latter). However, it is instructive to consider also the situation for conditions which are seriously relativistic but not as extreme as those for black holes and, for this purpose, we have made corresponding calculations for a sequence of spherically symmetric models each consisting of a constant-density central object surrounded by a vacuum, giving the linked Schwarzschild interior and exterior solutions. While it is clear that these models are not realistic representations of real astrophysical objects (such as neutron stars, for example), they are very useful for probing the effects of general relativity where it deviates significantly from Newtonian theory, particularly as they allow many calculations to be carried out analytically. In Sec. IV we present a series of figures showing the progressive changes in the shapes of the effective potential curves and von Zeipel cylinders as one proceeds from models which are only mildly relativistic to ones where the relativistic effects are overwhelming. Finally, in the concluding section, we draw together the interconnections between the different topics which we have been discussing.

<sup>1</sup>Abramowicz [1] proved that, under some particular conditions, von Zeipel cylinders must have cylindrical topology. However, further studies [2,3] showed that these conditions were overly restrictive and that cylindrical topology corresponds just to a particular case.

## II. DEFINITION OF CENTRIFUGAL FORCE IN GENERAL RELATIVITY

As mentioned above, we here restrict our attention to circular motion within a space-time which is static and axially symmetric and which therefore has two orthogonal Killing vector fields, which we will denote, respectively, by  $\eta^\alpha$  (timelike) and  $\xi^\alpha$  (spacelike). We use units in which  $c=G=1$  and adopt the spacelike signature convention  $(-, +, +, +)$ ;  $\nabla_\alpha$  denotes the covariant derivative in the space-time; greek indices are taken to run from 0 to 3.

First, we will give invariant definitions of various quantities which will be used in the subsequent discussion. The proper circumferential radii of circles whose symmetry axis corresponds to that of the space-time are given by

$$r = \sqrt{(\xi\xi)}, \quad (4)$$

and the “global” outward direction is that of the vector  $\nabla_\alpha r$ .

For general geodesic motion with four-velocity  $v^\alpha$ , there is one constant of the motion associated with each of the symmetries of the space-time: the energy  $\mathcal{E} = -\eta^\alpha v_\alpha$  and the angular momentum  $\mathcal{L} = \xi^\alpha v_\alpha$ . The quantity  $\bar{r}$  is constructed using  $\mathcal{E}$  and  $\mathcal{L}$  (whether or not the motion is geodesic) and also the angular velocity  $\Omega$ :

$$\bar{r} = \left[ \frac{\mathcal{L}}{\mathcal{E}\Omega} \right]^{1/2} = \left[ -\frac{(\xi\xi)}{(\eta\eta)} \right]^{1/2}. \quad (5)$$

It is defined to be strictly non-negative. The associated “local” outward direction is that of the vector  $\nabla_\alpha \bar{r}$ .

For circular motion of a test particle with a nonzero rest mass within the sort of space-time which we are considering, the four-velocity can be written as

$$v^\alpha = \frac{\eta^\alpha + \Omega \xi^\alpha}{\sqrt{-(\eta\eta) + \Omega^2(\xi\xi)}}, \quad (6)$$

and the acceleration  $a_\alpha \equiv v^\beta \nabla_\beta v_\alpha$  is given by

$$a_\alpha = \frac{1}{2} \frac{\nabla_\alpha(\eta\eta) + \Omega^2 \nabla_\alpha(\xi\xi)}{(\eta\eta) + \Omega^2(\xi\xi)}. \quad (7)$$

A *stationary observer* ( $\Omega \equiv 0$ ) with four-velocity

$$u^\alpha = \frac{\eta^\alpha}{\sqrt{-(\eta\eta)}} \quad (8)$$

uniquely defines a global rest frame and a projected three-space. The orbital speed in this projected three-space is

$$\bar{v} = \frac{\Omega \bar{r}}{\sqrt{1 - \Omega^2 \bar{r}^2}}. \quad (9)$$

Equation (7) can then be rewritten in the form

$$a_\alpha = \frac{1}{2} \nabla_\alpha \ln[-(\eta\eta)] - \frac{\bar{v}^2}{\bar{r}} \nabla_\alpha \bar{r}. \quad (10)$$

In order to keep the particle moving on its circular path, a force must in general be applied so as to produce the acceleration given by Eq. (10), except that in the special

case of geodesic motion this applied force goes to zero.

In Newtonian theory, where gravity appears as an applied force, we are used to thinking of the condition for motion on a free circular orbit as being given by the balance between gravity and the centrifugal force. Also, it is usual to describe the effect produced (for example) on passengers in a car which turns a sharp corner as being due to centrifugal force. There is no necessity for introducing the concept of centrifugal force in these cases (one could always talk in terms of the applied force producing an acceleration rather than of it acting against another force), but it has proved to be a very useful concept in analyzing physical situations. It is natural, therefore, to ask how an equivalent idea of centrifugal force could be introduced in general relativity. Here, there is the difference that gravity now appears as part of the acceleration, and so the question arises of how one should identify the “gravitational” and “centrifugal” parts of the acceleration vector. This question is controversial; in principle, there is not only one unique way to do it. Abramowicz [3] argued that since the gravitational force is normally thought of as being independent of velocity, the natural splitting consists of identifying the first term on the right-hand side of Eq. (10) as the “gravitational force per unit mass” and the second term as the “centrifugal force per unit mass.” For a particle with rest mass  $m_0$ , the centrifugal force is then given by

$$\mathcal{C}_\alpha = m_0 \frac{\bar{v}^2}{\bar{r}} \nabla_\alpha \bar{r}. \quad (11)$$

A consequence of this definition is that the centrifugal force always acts in the local outward direction (as given by  $\nabla_\alpha \bar{r}$ ) even if this becomes misaligned with the global outward direction (as given by  $\nabla_\alpha r$ ). In the vacuum Schwarzschild metric, the acceleration becomes independent of velocity on the circular photon orbit at  $r=3M$  ( $\nabla_\alpha \bar{r}$  is zero there), and interior to this the local and global outward directions are directly opposite for motion in the equatorial plane.

The approach leading to Eq. (11) has been criticized by de Felice [4] on the grounds that (i) he doubts the value of introducing the idea of centrifugal force into general relativity at all and (ii) if one is to introduce it then one should choose a definition which will keep it always pointing in a direction away from the axis of rotation. We take the view that the concept of centrifugal force is a valuable one to introduce into general relativity and that while it is certainly true that the definition is not unique, the simplicity and elegance of the formulas resulting from definition (11) and the formal unity to which it gives rise are powerful arguments in its favor. Also, the reversal of direction does not seem counterintuitive when viewed in the light of the fact that  $\mathcal{C}_\alpha$  is always aligned with  $\nabla_\alpha \bar{r}$ , which we have argued defines the local outward direction in the way relevant for consideration of the dynamical effects of rotation. Indeed, a definition of centrifugal force which did not have the property of always being aligned with  $\nabla_\alpha \bar{r}$  would appear to be counterintuitive. In the remainder of this paper, we will therefore use the term “centrifugal force” to mean the quantity defined by Eq. (11).

### III. EFFECTIVE POTENTIAL FOR PHOTON MOTION AND ITS RELATION TO THE RADIUS OF GYRATION

The connection between the behavior of centrifugal force and the location of the circular photon orbit in the vacuum Schwarzschild geometry suggests that circular photon orbits might in general play an important role in connection with rotational effects. This provides motivation for investigating the behavior of the *effective potential* for photon motion in general static space-times.

Using the condition  $(vv)=0$  for photon motion and defining  $V^\alpha$  to be the component of the photon four-velocity orthogonal to both  $\eta_\alpha$  and  $\xi_\alpha$ , one obtains

$$(VV) = -\frac{\mathcal{G}^2}{(\eta\eta)} - \frac{\mathcal{L}^2}{(\xi\xi)}, \quad (12)$$

which can be rearranged to give

$$-\frac{(\eta\eta)}{\mathcal{L}^2} (VV) = \frac{\mathcal{G}^2}{\mathcal{L}^2} - \mathcal{V}_{\text{eff}}^2, \quad (13)$$

where the left-hand side is strictly non-negative and  $\mathcal{V}_{\text{eff}}$  is the effective potential for photon motion,<sup>2</sup> given by

$$\mathcal{V}_{\text{eff}} = \left[ -\frac{(\eta\eta)}{(\xi\xi)} \right]^{1/2}. \quad (14)$$

A remarkable consequence of Eq. (14) is that

$$\mathcal{V}_{\text{eff}} = \frac{1}{\bar{r}} \quad (15)$$

(we define it to be positive), giving

$$\mathcal{C}_\alpha = -m_0 \bar{v}^2 \bar{r} \nabla_\alpha \mathcal{V}_{\text{eff}}. \quad (16)$$

The equipotential surfaces for photon motion precisely coincide with the level surfaces of  $\bar{r}$  (the von Zeipel cylinders), and the direction of the centrifugal force  $\mathcal{C}_\alpha$  (which is the direction of increase of  $\bar{r}$ ) is the direction of decrease of  $\mathcal{V}_{\text{eff}}$ . Circular photon orbits occur at local extrema of the effective potential, with maxima corresponding to unstable orbits and minima to stable ones. The centrifugal force is zero on circular photon orbits and, in the equatorial plane, always points away from unstable ones and towards stable ones. In the next section, we illustrate these features for a particular case.

<sup>2</sup>Note that in the literature there are two different conventions for the definition of  $\mathcal{V}_{\text{eff}}$ , one being that used here and the other defining  $\mathcal{V}_{\text{eff}}$  to be the square of the present quantity. For the purposes of this paper there is no particular advantage of adopting one convention rather than the other, but the one used here is definitely preferable when the treatment is extended to general stationary space-times. In a preliminary report on the present work [7], the alternative convention was used, and so there are some small differences in formulas and graphs between that paper and the present one.

#### IV. EFFECTIVE POTENTIAL CURVES AND VON ZEIPEL CYLINDERS FOR THE INTERIOR AND EXTERIOR SCHWARZSCHILD METRICS

As mentioned in the Introduction, the equatorial effective-potential curve and the structure of the von Zeipel cylinders are already well known for the case of Schwarzschild black holes. Here, we want to investigate the situation for objects which are not as extreme as black holes and which will provide a link between the familiar Newtonian conditions and the extreme relativistic ones. For this purpose, we have carried out a study of space-times generated by nonrotating spheres of matter with constant density and surrounded by vacuum (giving the linked Schwarzschild interior and exterior solutions). We have examined a sequence of models with progressively increasing degrees of compactness, and these can be seen as representing a quasistationary contraction. The models are very simple but provide a useful probe of the effects being considered.

For both the interior and exterior solutions, we write the metric in the standard form

$$ds^2 = -e^{2\nu} dt^2 + e^{2\lambda} dR^2 + R^2(d\theta^2 + \sin^2\theta d\phi^2), \quad (17)$$

where  $(t, R, \theta, \phi)$  are spherical polar coordinates. Interior to the matter,

$$e^{2\nu} = \frac{1}{4} \left\{ 3 \left[ 1 - \frac{2M}{R_*} \right]^{1/2} - \left[ 1 - \frac{2M}{R_*} \left( \frac{R}{R_*} \right)^2 \right]^{1/2} \right\}^2, \quad (18)$$

$$e^{2\lambda} = \left[ 1 - \frac{2M}{R_*} \left( \frac{R}{R_*} \right)^2 \right]^{-1}, \quad (19)$$

where  $M$  is the total mass of the sphere and  $R_*$  is its radius, while the external solution is

$$e^{2\nu} = e^{-2\lambda} = 1 - \frac{2M}{R}. \quad (20)$$

The squared lengths of the Killing vectors are then

$$(\eta\eta) = -e^{2\nu} \quad \text{and} \quad (\xi\xi) = R^2 \sin^2\theta, \quad (21)$$

so that

$$\tilde{r} = \begin{cases} \frac{2R \sin\theta}{3\sqrt{1-2M/R_*} - \sqrt{1-(2M/R_*)(R/R_*)^2}}, & R \leq R_*, \\ \frac{R \sin\theta}{\sqrt{1-2M/R}}, & R \geq R_*. \end{cases} \quad (22)$$

In the equatorial plane,  $R$  coincides with  $r$  as defined by Eq. (4).

The results for our sequence of models are presented in Figs. 1–5, which are drawn for a succession of decreasing values of  $R_*/2M$ . For each model we show (a) the curve of the photon effective potential ( $\mathcal{V}_{\text{eff}} = 1/\tilde{r}$ ) in the equatorial plane as a function of radius  $r$  and (b) a cross section through the von Zeipel cylinders in the plane containing the radial direction and the rotation axis [the drawings have been constructed in terms of the standard Schwarzschild coordinates of Eq. (17)]. The dashed line in the von Zeipel diagrams marks the surface of the sphere; interior to this there is matter with a constant density; exterior to it, there is vacuum. The cylinders have been drawn at equal spacing in  $\tilde{r}$ . We note that our results are exactly the lowest-order ones for the sequence of slowly rotating models studied by Chandrasekhar and Miller [8] and hence are supplementary to the results presented in that earlier paper.

For  $R_*/2M = 2.0$  (Fig. 1), the effective-potential curve differs only very slightly from the equivalent Newtonian one (a rectangular hyperbola), but a more obvious difference is seen for the von Zeipel cylinders. The ones with the largest radii are near to being straight cylinders, but those with smaller radii are pulled significantly inwards in the vicinity of the equatorial plane. For  $R_*/2M = 1.5$  (Fig. 2), the value at which the circular photon orbit of the vacuum Schwarzschild space-time is coincident with the surface of the sphere, the effective-potential curve has developed a stationary point (an

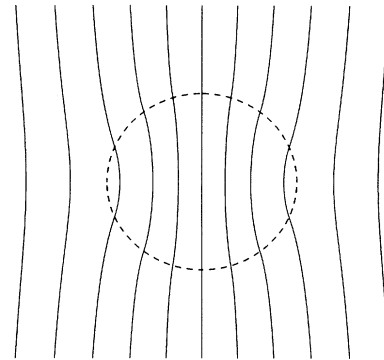
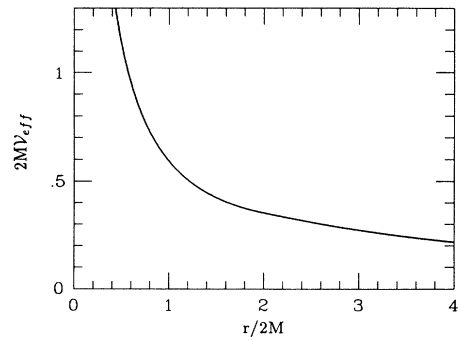
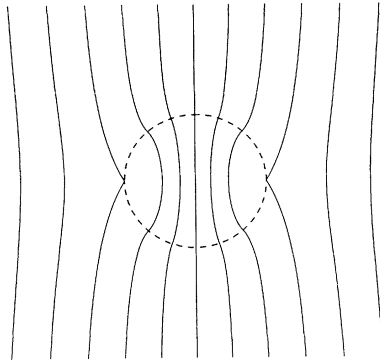
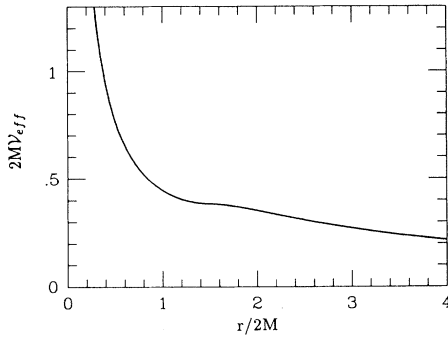
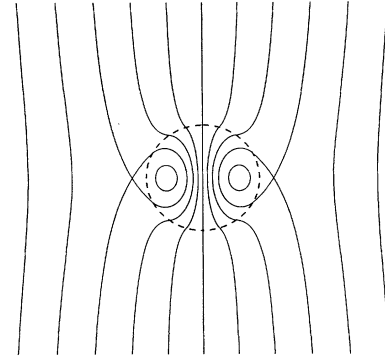
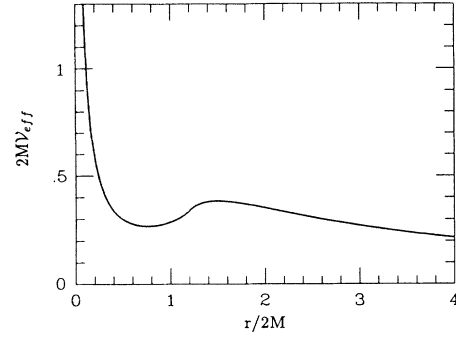


FIG. 1. The equatorial photon effective-potential curve for  $R_*/2M = 2.0$  and a cross section through the corresponding von Zeipel cylinders in a plane containing the rotation axis.

FIG. 2. The equivalent of Fig. 1 for  $R_*/2M = 1.5$ .FIG. 3. The equivalent of Fig. 1 for  $R_*/2M = 1.2$ .

inflection) at  $r = 3M$  and the centrifugal force has gone to zero there. The von Zeipel cylinder which touches the sphere at the equator has developed a cusp at which the normal vector has zero length.

For models which are more compact than this, a special role is played by the cylinder which intersects the equatorial plane at the unstable photon orbit (having  $r = 3M$  and  $\bar{r} = \bar{r}_c = 3\sqrt{3}M$ ), since this separates regions with different regimes of behavior. Each of the von Zeipel diagrams shows cylinders with  $\bar{r}$  ranging from  $\bar{r}_c/3$  to  $5\bar{r}_c/3$  in equal intervals of  $\bar{r}_c/3$ . For  $R_*/2M = 1.2$  (Fig. 3), the effective-potential curve has developed a clear minimum corresponding to a stable circular photon orbit internal to the matter. The existence of these stable orbits was first demonstrated and discussed by de Felice [9]. They are located at

$$\frac{R}{R_*} = \frac{2\sqrt{2}}{3} \left[ \frac{R_*}{2M} \frac{R_* - 9M/4}{R_* - 2M} \right]^{1/2}, \quad (23)$$

and, after their first appearance at the equator when  $R_* = 3M$ , they move progressively inwards through the matter region (in the sense of decreasing  $R/R_*$ ) as  $R_*$  is further reduced. The unstable circular photon orbit in the vacuum region remains at  $R = 3M$ . Recalling that  $\bar{r}$  increases when  $\mathcal{V}_{\text{eff}}$  decreases, one sees that, in the equatorial plane, the local and global outward directions become opposite inbetween the two circular photon orbits but coincide elsewhere. The centrifugal force, which is always aligned with the local outward direction, becomes globally inward pointing in the equatorial plane between

the two circular photon orbits.

The central part of the diagram for the von Zeipel cylinders has become rather complicated by  $R_*/2M = 1.2$ , and it is helpful to consider each of the cylinders separately for this case. Figure 4 shows first the equatorial photon effective-potential curve with horizontal dashed lines marking the magnitude of  $\mathcal{V}_{\text{eff}}$  on each of the cylinders. The other frames of the figure then show the cross sections through each of the cylinders in turn. For the lowest dashed line (corresponding to the outermost cylinder having  $\bar{r} = 5\bar{r}_c/3$ ) there is only one point of intersection of the dashed line with the curve and hence only one value of  $r$  for which the cylinder intersects the equatorial plane. This cylinder is nearly Newtonian but bends inwards slightly near to the equatorial plane. Moving upwards, the next dashed line (corresponding to the cylinder with  $\bar{r} = 4\bar{r}_c/3$ ) has three points of intersection with the curve, and hence there are three values of  $r$  at which the equatorial plane is crossed. This ‘‘cylinder’’ has an outer part with normal cylindrical topology but also a disconnected inner part with toroidal topology. The dynamical outward normal vectors  $\nabla_\alpha \bar{r}$  point towards the exterior of the part with cylindrical topology but towards the interior of the toroidal section. This is a general behavior. As one moves to cylinders with decreasing  $\bar{r}$ , the toroidal section first appears as a torus of zero thickness coinciding with the stable circular photon orbit. Moving up again, the third dashed line (corresponding to the critical cylinder with  $\bar{r} = \bar{r}_c$ ) intersects the curve at two points, and so there are two values of  $r$  at which the equatorial plane is crossed. The section with

toroidal topology has now expanded and joins the part with a cylindrical topology at the cusp (at  $r = 3M$ ). The directions of  $\nabla_{\alpha}\tilde{r}$  follow the behavior described above. For the next dashed line ( $\tilde{r} = 2\tilde{r}_c/3$ ), there is again only a single point of intersection with the curve and the toroidal region has reconnected with the cylindrical one giving a strictly cylindrical topology throughout. Finally, we show the innermost cylinder (with  $\tilde{r} = \tilde{r}_c/3$ ), which corresponds to the top dashed line.

Returning to our sequence of models with decreasing  $R_*/2M$ , Fig. 5 shows the situation for the most compact possible equilibrium model, which has  $R_*/2M = 1.125$ . (The central pressure is infinite in this case.) Here, the minimum in the effective-potential curve has moved to  $r = 0$ ; all cylinders with  $\tilde{r}_c \leq \tilde{r} < \infty$  have both outer and inner sections and the holes in the middle of the tori have closed up. (Note that only the cylinders with our five

chosen values of  $\tilde{r}$  have been illustrated here. The innermost torus shown is completely filled by a family of further tori which are the counterparts of the family of outer cylindrical sections stretching out to infinity.) Finally, in Fig. 6 we show the corresponding situation for a Schwarzschild black hole with the dashed line on the von Zeipel diagram here marking the position of the event horizon ( $R_*/2M = 1.0$ ). Now, all of the cylinders have been expelled from the interior of the event horizon, and those with  $\tilde{r} \geq \tilde{r}_c$  consist of an outer part with cylindrical topology and an inner part with spheroidal topology which is tangential to the event horizon at the poles. As  $\tilde{r} \rightarrow \infty$ , the inner spheroidal region becomes closer and closer to being exactly coincident with the event horizon. For  $\tilde{r} < \tilde{r}_c$ , the cylinders form two disconnected parts, one above the equatorial plane and one below it, with each part being closed off at  $R = 2M$ , where it becomes tangen-

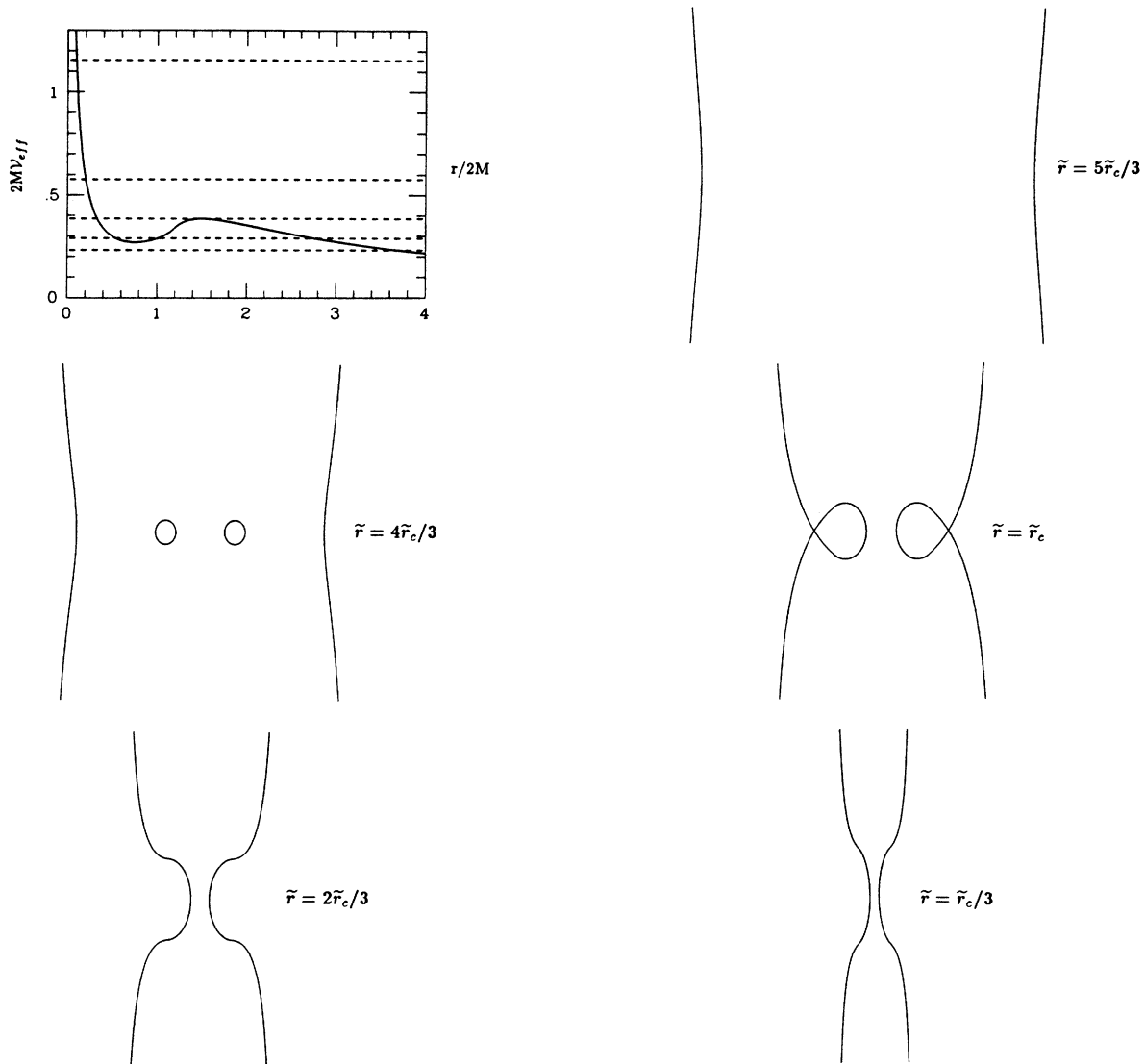


FIG. 4. Individual von Zeipel cylinders for the case  $R_*/2M = 1.2$ . See text for details.

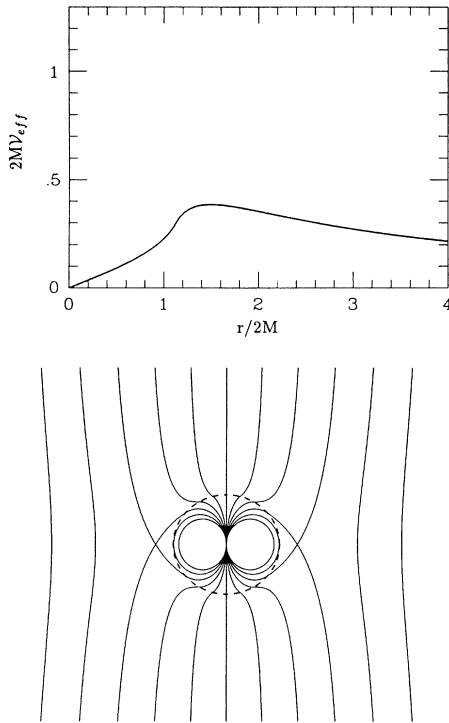


FIG. 5. The equivalent of Fig. 1 for  $R_*/2M = 1.125$ .

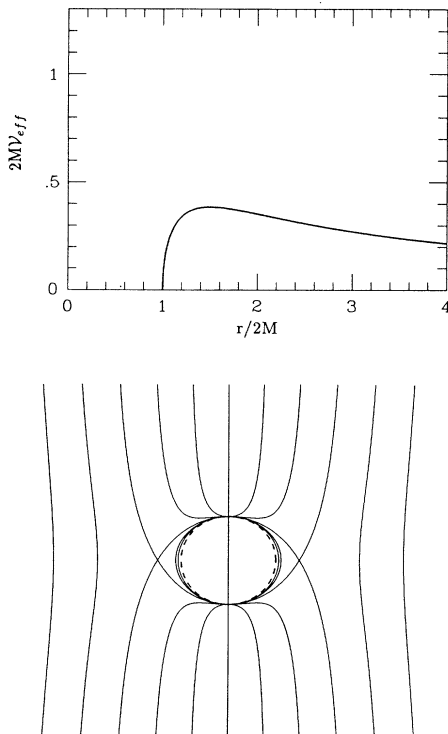


FIG. 6. The equivalent of Fig. 1 for a Schwarzschild black hole.

tial to the event horizon at the poles in the same way as the spheroidal sections. Following the behavior described earlier,  $\nabla_{\alpha}\tilde{r}$  points towards the exterior of the topologically cylindrical sections (and also of the cylindrical sections which are broken in the middle for  $\tilde{r} < \tilde{r}_c$ ) but towards the interior of the spheroidal sections.

## V. DISCUSSION AND CONCLUSION

In this paper, we have focused on the role of the radius of gyration  $\tilde{r}$  as the dynamically important radial quantity for discussion of rotational properties. It has its origin in the link between specific angular momentum and angular velocity; its gradient defines the local outward direction relevant for discussion of the dynamical effects of rotation; its level surfaces are the von Zeipel cylinders which are found also to correspond to the equipotential surfaces of the effective potential for photon motion. Our definition of centrifugal force in general relativity is made in terms of the radius of gyration, and while this definition depends to some extent on personal taste, we argue that our choice is a particularly favored one.

The origin of this definition of centrifugal force comes from the paper by Abramowicz, Carter, and Lasota [10], who carried out their discussion in terms of the *optical reference geometry*, a conformal adjustment of the projected three-space introduced in Sec. II in which the geodesic lines are the spatial projections of photon trajectories. Up to this point, we have purposely not made any reference to this in the present paper, but it is now worth pointing out that the radius of gyration  $\tilde{r}$  is also precisely the proper circumferential radius in the optical reference geometry. Also, the fact that the von Zeipel cylinders and the equipotential surfaces for photon motion coincide is an indication of the underlying interconnection which exists.

Study of the distortion of the von Zeipel cylinders in strong fields gives some valuable insight into rotational effects in general relativity. Abramowicz and Miller [11] demonstrated how, within the present framework, it is possible both to make a surprisingly accurate analytical calculation of a strong-field rotational effect and also to get an improved conceptual understanding of why it occurred. The phenomenon studied there was the following. If one takes an axisymmetric constant-density object in uniform rotation (a Maclaurin spheroid) and considers a quasistationary contraction in which the total mass and angular momentum are conserved, then within Newtonian theory one expects that (assuming axisymmetry is maintained) the object will spin progressively faster and become progressively more flattened, eventually ending as a thin disc. When general relativistic corrections to Newtonian theory need to be taken into account, the situation becomes more complicated. Chandrasekhar and Miller [8] made a corresponding calculation for Maclaurin spheroids in full general relativity, but within the slow-rotation regime, and found that as the contraction proceeds the object first becomes progressively more flattened (consistently with the Newtonian calculations) but that the flattening reaches a maximum at  $R_*/2M \approx 2.5$  and subsequent further contraction would lead to the ob-

ject becoming more spherical again. Abramowicz and Miller demonstrated that this behavior can be reproduced to high accuracy with an analytic calculation using Newtonian equations modified so as to follow relativistic definitions of angular momentum and centrifugal force.<sup>3</sup> Now it can be seen that the two types of correction introduced there are closely interrelated; both result from distortion of the von Zeipel cylinders. (While dragging of inertial frames is an important phenomenon in other contexts, it is not responsible for the reversal of ellipticity.) Also, the relative increase in moment of inertia of compact configurations (as shown by Fig. 2 of the paper by

Chandrasekhar and Miller [8]) is directly connected with this distortion.

We have restricted attention here to static, axially symmetric space-times but, of course, eventually the main interest is in more general situations. As mentioned previously, the extension to stationary space-times has already been completed, and extension to completely general space-times is currently under investigation.

#### ACKNOWLEDGMENTS

Z.S. would like to express his gratitude to Dr. J. A. Edgington for hospitality at Queen Mary & Westfield College, London and to the Commission of the European Communities for financial support within the framework of the TEMPUS scheme. J.C.M. acknowledges financial support from the Italian Ministero dell'Università e della Ricerca Scientifica e Tecnologica.

---

<sup>3</sup>We point out that we are in disagreement with the analysis made recently by Chakrabarti and Khanna [12] which we believe to be incorrect. We will discuss this in detail elsewhere.

- 
- [1] M. A. Abramowicz, *Acta Astron.* **24**, 45 (1974).
  - [2] M. A. Abramowicz, *Astrophys. J.* **254**, 748 (1982).
  - [3] M. A. Abramowicz, *Mon. Not. R. Astron. Soc.* **245**, 733 (1990).
  - [4] F. de Felice, *Mon. Not. R. Astron. Soc.* **252**, 197 (1991).
  - [5] M. A. Abramowicz, *Mon. Not. R. Astron. Soc.* **254**, 710 (1992).
  - [6] S. L. Shapiro and S. A. Teukolsky, *Black Holes, White Dwarfs, and Neutron Stars: The Physics of Compact Objects* (Wiley, New York, 1983), p. 350.
  - [7] J. C. Miller, in *Approaches to Numerical Relativity*, edited

- by C. J. S. Clarke and R. d'Inverno (Cambridge University Press, Cambridge, England, 1992).
- [8] S. Chandrasekhar and J. C. Miller, *Mon. Not. R. Astron. Soc.* **167**, 63 (1974).
- [9] F. de Felice, *Nuovo Cimento B* **63**, 649 (1969).
- [10] M. A. Abramowicz, B. Carter, and J. P. Lasota, *Gen. Relativ. Gravit.* **20**, 1173 (1988).
- [11] M. A. Abramowicz and J. C. Miller, *Mon. Not. R. Astron. Soc.* **245**, 729 (1990).
- [12] S. K. Chakrabarti and R. Khanna, *Mon. Not. R. Astron. Soc.* **256**, 300 (1992).